

PACS numbers: 07.85.Fv; 41.50.+h; 42.55.Vc; 85.40.Hp
DOI: 10.1070/QE2002v032n12ABEH002354

Multilayer X-ray optics

A.V. Vinogradov

***Abstract*. The principles, state of the art, and problems of multilayer X-ray optics are analysed. Among its applications, the projection X-ray lithography and mirrors for a repetitively pulsed capillary-discharge X-ray laser are considered.**

Keywords: *X-ray optics, X-ray lasers, projection X-ray lithography*.

1. Introduction

The use of lasers for creating a high-temperature plasma proposed by N.G. Basov and O.N. Krokhin [1] has given a powerful impulse to investigations in several fields of physics (the state of the art and history of studies of laser fusion are presented in [2]). Among these are X-ray spectroscopy and physics of highly ionised atoms. Within a short period of time, high-power laser facilities were built at the P.N. Lebedev Physics Institute (LPI), Russian Academy of Sciences (RAS), and other research centres, at which a large amount of experimental data on the properties and X-ray spectra of multiply charged ions were obtained [3, 4]. The advent of such a unique radiation source as a laser plasma evoked an additional interest in X-ray physics and designing X-ray lasers. At that time, single-pass systems for generating laser radiation, such as laser diodes or free-electron lasers, did not exist, and a laser of practical importance without a resonator could be hardly conceived. However, in contrast to experimental studies on active media, which began in 1971 [5], the number of publications on X-ray resonators was small (e.g., [6]).

The concept of multilayer X-ray mirrors was proposed at the sector headed by I.I. Sobel'man within the laboratory headed by N.G. Basov [7] as an attempt to solve an urgent problem of X-ray laser resonators [8]. Such mirrors were proposed earlier for space explorations [9]. Some time later, multilayer X-ray mirrors became widely used elements in devices of laboratory and industrial microanalysis and in solar investigations. At the same time, it occurred, that, for some reasons, resonators are seldom used to obtain lasing in modern X-ray lasers. However, multilayer X-ray mirrors are extremely necessary for their development and application.

A.V. Vinogradov P.N. Lebedev Physics Institute, Russian Academy of Sciences, Leninskii prosp. 53, 119991 Moscow, Russia;
e-mail: vinograd@sci.lebedev.ru

Received 23 September 2002
Kvantovaya Elektronika **32** (12) 1113 – 1121 (2002)
Translated by A.S. Seferov

This paper analyses the state of the art and the main problems of multilayer X-ray optics. Much attention is paid to the projection X-ray lithography and mirrors for X-ray lasers. Both of these trends were developed at the Department of Quantum Radiophysics headed by N.G. Basov.

The X-ray lithography method, in which the image of a mask is transferred to the surface of a silicon wafer by a system of multilayer mirrors of normal incidence, is now regarded as the most probable basis for the technology of manufacturing integrated microcircuits of the next generation.

The creation of a high-power repetitively pulsed radiation source emitting at 46.9 nm [10] is an outstanding achievement of laser physics of the recent decade. At present, this laser is the brightest source of short-wavelength radiation and is used in interferometry, reflectometry, and other fields. The development of efficient optical elements for a 46.9-nm repetitively pulsed laser is of special interest also in connection with the rapid development of lasers at shorter wavelengths (10 – 20 nm) and free-electron lasers [11].

2. Selection of materials for X-ray optics

The main factor that restricts the reflectivity of multilayer mirrors for soft X-rays is the fundamental absorption. The reflectivity can be optimised by selecting the materials and layer thicknesses. In particular, for a pair of materials 1 and 2, the optimal layer thicknesses l_1 and l_2, at which the reflectivity R for a semi-infinite 121212.... structure synthesised from these two materials is maximum, were found in [7] in terms of the permittivities ε_1 and ε_2 of these materials by solving the equations of wave propagation in a periodical structure. For the normal incidence, the results are:

$$
\begin{aligned}
&2l = \lambda\left[\mathrm{Re}\,\bar{\varepsilon} - \frac{\sin(2\pi\beta)}{2\pi}\,\mathrm{Im}\Delta\varepsilon\right]^{-1/2}, \quad \bar{\varepsilon} = \beta\varepsilon_1 + (1-\beta)\varepsilon_2,\\
&\tan\pi\beta = \pi\left(\beta + \frac{\mathrm{Im}\varepsilon_1}{\mathrm{Im}\Delta\varepsilon}\right), \quad \beta = \frac{l_1}{l}, \quad \Delta\varepsilon = \varepsilon_2 - \varepsilon_1,\\
&R = \frac{1-\sqrt{u}}{1+\sqrt{u}},\\
&u = [1-\cos^2(\pi\beta)]\left[1 + \left(\frac{\mathrm{Re}\Delta\varepsilon}{\mathrm{Im}\Delta\varepsilon}\right)^2\cos^2(\pi\beta)\right]^{-1}.
\end{aligned}
\tag{1}
$$

Here, $l = l_1 + l_2$ is the period of the structure and $\bar{\varepsilon}$ is the average permittivity. Expressions (1) show that the optimal reflectivity depends on the ratio of constants rather than on their absolute values. Therefore, unlike the case of a reflection from a single interface, the reflectivity is not a small value. The basic requirements for the material selection follow from (1) [12].

Other approaches to the optimal selection of materials for high-reflectivity multilayer mirrors also exist (e.g., [13, 14]). In any case, in the first approximation, it can be considered that the most favourable pair of materials must have a minimum absorption and a maximum difference in the refractive indices (i.e., the real parts of the permittivities). From this viewpoint, the two most widespread features of the absorption spectrum of the reflecting material are of interest: a clearly pronounced resonance (or a line, Fig. 1) and absorption jumps or edges corresponding to the ionisation potentials of the K, L, M... electron shells (Fig. 2).*

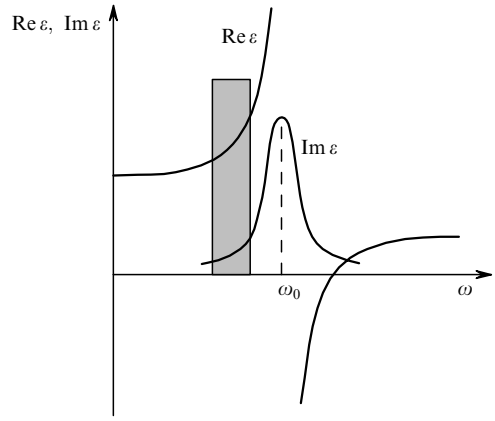

Figure 1. Typical frequency dependence of the optical constants of a material in the presence of an absorption line.

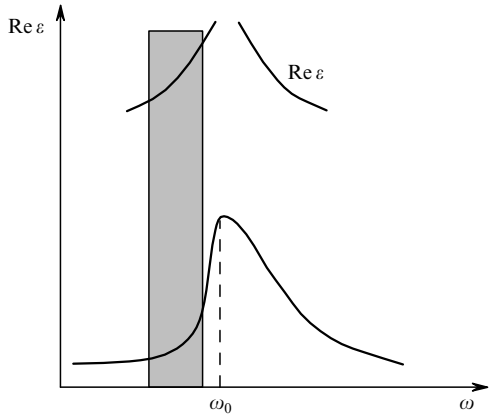

Figure 2. Typical frequency dependence of the optical constants of a material in the presence of a photoabsorption jump.

*Other types of photoabsorption features are the Fano resonances, the Cooper dip, a near-threshold structure, peculiarities related to plasma oscillations, etc. However, their influence on $\mathrm{Re}\,\varepsilon$ and the optical properties of multilayer structures was poorly studied (see, however, [15–18]).

The behaviour of $\mathrm{Re}\,\varepsilon$ near these singularities can be easily understood using the Kramers–Kronig relations. In the case of an absorption line, $\mathrm{Re}\,\varepsilon$ has a maximum, as in the visible range, located close to the resonance and slightly shifted to the red with respect to the resonance peak. In the case of a photoabsorption jump, $\mathrm{Re}\,\varepsilon$ has a logarithmic singularity: $\mathrm{Re}\,\varepsilon \sim \Delta\mathrm{Im}\,\varepsilon \cdot \ln|\omega - \omega_0|$, where $\Delta\mathrm{Im}\,\varepsilon$ is the jump magnitude and ω_0 is its position.

In fact, in both cases presented in Figs 1 and 2, there exists a frequency range with a low absorption ($\mathrm{Im}\,\varepsilon$) and high refraction ($\mathrm{Re}\,\varepsilon$) (shaded rectangles). The most detailed analysis of elements and chemical compounds from the viewpoint of their application as components of multilayer X-ray mirrors was performed in [19].

Another aspect of this problem is the compatibility of the selected pair of materials from the viewpoint of their ability to form sufficiently sharp and smooth (along the layers) interfaces, which must be reproduced in structures containing tens and hundreds of layers. Numerous special studies were devoted to this problem. The relevant references can be found in [12, 25, 29, 31] and in an excellent review by T.W. Barbee [*Opt. Eng.*, **35**, 899 (1986)].

3. State of the art and problems of multilayer optics

Figs 3 and 4 from [20] present the layer materials and the reflectivities of multilayer X-ray mirrors at glancing angles of 90° and 45° with respect to the surface. At glancing angles close to 45°, the contribution of p-polarisation to the reflectivity is very small. This is used in the manufacturing of polarisation elements (see [21, 22] and, in more detail, [23, 31]). In the case of a normal incidence, the highest reflectivity is 70 % at $\lambda = 13$ nm and it becomes below 10 % at $\lambda \leqslant 4$ nm. For comparison, the reflectivity of any massive material is no higher than 10 % at $\lambda = 40$ nm and 0.1 % at $\lambda < 4$ nm.

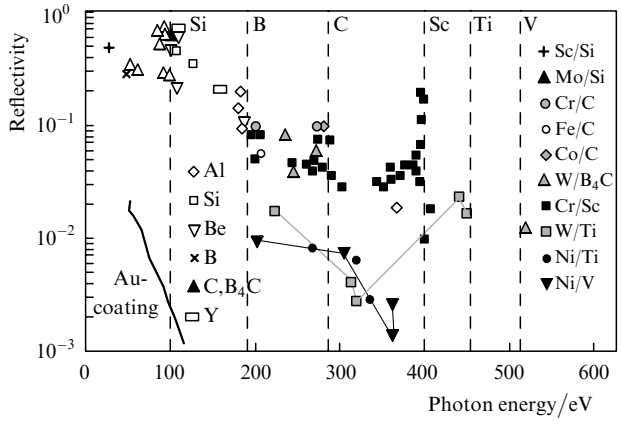

Figure 3. Reflectivity of multilayer mirrors at the normal incidence for various pairs of materials [20].

The most important practical problem of multilayer optics is *an advance to shorter wavelengths* ($\lambda \approx 3$–6 nm). The matter is that the carbon photoabsorption edge lies in this spectral region ($\lambda \approx 4.4$ nm). A study of the structure of the absorption or emission spectrum near this edge is one of the main tools for investigating carbon-

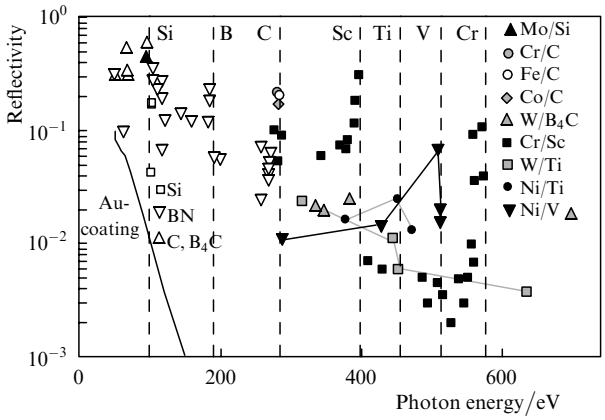

Figure 4. Reflectivity of multilayer mirrors at an angle of incidence of 45° for various pairs of materials [20].

containing materials, such as polymers, carbides, hydrocarbons, nanotubes, diamond-like films, graphites, living tissues, etc. The development of focusing and dispersing optics for this spectral region would contribute to the creation of new extremely necessary instruments. However, the reflectivities of multilayer X-ray mirrors at $\lambda \approx 3-6$ nm are still 2–3 times lower than the theoretical values, and this substantially limits the possibilities of their application. The causes of this discrepancy are related to various defects in reflecting periodic coatings, whose influence at $\lambda < 3$ nm becomes dramatic: the reflectivity at the normal incidence decreases to a few percent and less. Hence, the modern technology does not ensure the required quality of multilayer structures in the short-wavelength region. According to the conventional concepts, the interfaces must be smooth along the layers, and a layer-to-layer transition in an ideal case must be stepwise. However, this is not observed in reality.

For clearness, let us make some estimates. The thickness l of one layer, the number N of pairs of layers, at which the reflectivity approaches a saturation, and the spectral width $\Delta\lambda/\lambda$ of the reflection are estimated from expressions

$$l \approx \frac{\lambda}{4}, \quad N \approx \frac{1}{\Delta\varepsilon}, \quad \frac{\Delta\lambda}{\lambda} \approx \frac{1}{N} \approx \Delta\varepsilon, \tag{2}$$

where $\Delta\varepsilon$ is the difference of the permittivities of the materials composing the multilayer structure. Using the data from [24], for 3-nm radiation, we obtain $l \approx 0.7$ nm and $N \approx 300$. With a further decrease in the wavelength, the layer thickness l approaches a limit determined by the interatomic distances, and the number of pairs of layers increases: $N \approx 1/\Delta\varepsilon \approx 1/\lambda^2$. No commercial equipment for depositing optical coatings of this type exists.

The state of the interface depends on the diffusion of the materials of adjacent layers and on the interaction between them. Chemical and phase transformations in multilayer structures are enhanced under the influence of thermal and radiation effects [25]. This leads to a degradation of the reflectivity, which is very important for space applications and for the case of multilayer optics developed for free-electron lasers. *The problems of thermal and radiation stability* of mirrors are solved by using special (often, refractory) materials, alloys, silicides [26], carbides, oxides, etc.; in addition, antidiffusion barriers are placed between the layers of the structure [27]. In particular, the operating temperature of a CrB_2/C multilayer mirror at a wavelength of 4.47 nm reached 900 °C [28]. At $T > 1100$ °C, the reflectivity degraded. These problems were investigated in [25, 29, 30].

Multilayer mirrors occupy a firm position in instruments for microanalysis, where they operate as selective reflectors and are also used to select characteristic emission lines of various elements (see details in [31, 32]). Studying the properties of magnetic and anisotropic materials in the soft X-ray region requires polarisation elements, polarisers and phase shifters. In this case, no alternative to multilayer coatings exists [23, 31].

When developing new methods and instruments for enhancing the sensitivity and signal-to-noise ratio, apart from the necessity of increasing the reflectivity of mirrors, there is a problem of synthesising coatings with an extremely narrow reflection band. This is achieved by selecting the materials with a certain ratio of optical constants and optimising the layer thicknesses [12]. One of the possibilities is the deposition of carbon–carbon coatings. This means that both components of the structure are carbon (or a hydrocarbon), and its alternate layers have different densities [33, 34]. In some cases (microanalysis, astrophysics), on the contrary, it is desirable to extend the reflection band or attain a high reflectivity at two wavelengths. The problem of *synthesising a coating with a specified reflectivity* as applied to X-ray optics was considered in [35–40]. A detailed analysis and the history of this issue are presented in [41]. During manufacturing of such mirrors, difficulties appear that are associated with the control of the layer thickness and tests of multilayer aperiodic coatings.

A sufficiently high reflectivity makes it possible to construct *imaging optical systems of normal incidence* consisting of two and a larger number of mirrors and, due to a cancellation of geometrical aberrations, to achieve a high spatial and angular resolution, which, in an ideal case, is determined by the diffraction limit. Several generations of three-mirror X-ray microscopes for obtaining images of nonluminous objects were developed in joint investigations of the LPI, General Physics Institute, and Kharkov Polytechnical Institute [42–46] (Fig. 5). One of the mirrors served as a condenser and concentrated the radiation from a laser-plasma source at the object under study. Two other mirrors composed a Schwarzschild objective. An image is obtained in a single laser shot at a pulse energy of ~ 0.2 J. At present, the resolution of these systems is no better than 0.2 μm, which is approximately three times worse than the diffraction-limited resolution.* The same microscope was used for visualising filtration channels in polymer membranes [48, 49]. In this case, the laser-plasma source was formed using a repetitively pulsed laser with a pulse energy of ~ 0.1 J.

The problem of *reaching the diffraction limit* in X-ray optics is related not only to the quality of coatings but, probably, to a higher degree, to the accuracy of the shapes of substrates and their smoothness. The greatest progress has been achieved in the range of 13–17 nm, where the reflectivity is maximum (~ 70 %, see Fig. 3) and agrees with

*It was shown in [45, 47] that the highest possible ray-optical resolution of the Schwarzschild objective can reach 0.02 μm. This value is not attained in practice because of inaccuracies in the mirror profile and diffraction effects.

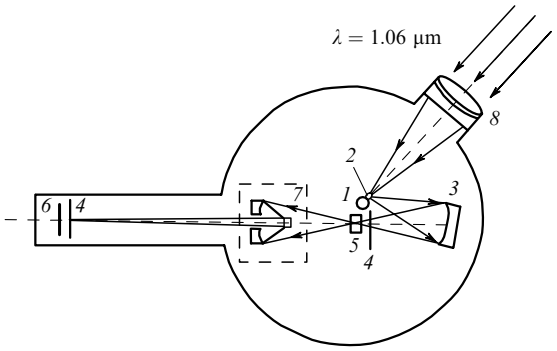

Figure 5. Schematic of an X-ray microscope containing three mirrors with multilayer coatings: (*1*) rhenium target; (*2*) laser flame; (*3*) condenser mirror; (*4*) aluminium filters; (*5*) object under study; (*6*) photographic film; (*7*) two-mirror X-ray Schwarzschild objective; and (*8*) laser-beam-focusing lens.

the theoretical value. The angular resolution of Sun images in this spectral region exceeds $1''$ (730 km on the solar surface) [50], making it possible to study the dynamics and nature of solar magnetic structures.* A telescope–spectrometer, which is projected to be set in operation in 2005, will allow researchers to obtain their images with a spectral resolution $\Delta\lambda/\lambda \leqslant 10^{-4}$ [54]. In projection X-ray lithography systems, images of micromasks containing elements with dimensions of 0.05–0.07 μm were obtained in the same spectral region [23, 55]. This question will be discussed below.

While a wavelength of 3 nm is now a limit for the optics of normal incidence, in the case of an oblique incidence, multilayer optics is also successfully used with hard X rays ($\lambda \leqslant 0.2$ nm). Such radiation is generated by X-ray tubes and is widely applied in research and industrial equipment. The use of multilayer coatings on bent substrates makes it possible to focus the radiation at the objects under study, thus appreciably extending the capabilities of X-ray tubes. The methods developed in this field and the corresponding results are presented in the Proceedings of Symposiums on X-ray Optics arranged by the Institute of Microstructure Physics of RAS (Nizhnii Novgorod) [56, 88].

4. Projection X-ray lithography

A successful development of this field will provide the extensive applications of multilayer X-ray optics, since we deal with microelectronics, namely, with the production of a new generation of microcircuits with sizes of elements of 0.07–0.03 μm.** It is obvious that, at such a scale, the micromask imaging onto the surface of a silicon wafer can be produced only with X-rays. The complexity of designing the optical systems for X-ray lithography involves the necessity of simultaneously ensuring a high spatial resolution and a large field of view. This results in an increased number of optical elements in the imaging system.

As was already mentioned, the highest reflectivity of $\sim 70\,\%$ was obtained at $\lambda \sim 13$ nm. This wavelength was selected for implementing ambitious projects on projection X-ray lithography (Extreme Ultraviolet Lithography, EUVL), which have a status of Federal and International Programs in the USA, Japan, and the EU. At N.G. Basov's laboratory the first project named 'Projection X-ray Lithography' ('Karat') was carried out in 1989–1991 and financed by the HTSC Council of the RAS. Earlier, N.G. Basov recommended the publication of paper [57] in which it was concluded that a resolution of $\sim 0.1 - 0.01$ μm can be achieved using the projection X-ray lithography method (see also [58, 59]).

The projection X-ray lithography imposes extremely high requirements on multilayer X-ray mirrors. It is expedient to discuss some of them, although they may be not so stringent for other applications. Consider the accuracy of manufacturing substrates (Table 1), since the interfaces of a growing structure usually inherit the shape of the substrate surface. Two types of a deviation of the substrate surface from a required ideal shape, which can be either spherical or aspherical, are distinguished: roughnesses (small-scale deviations) and large-scale shape deviations.

A roughness leads to scattering and, consequently, reduces the intensity of a specularly reflected beam, which is often absolutely intolerable, especially if we deal with the projection X-ray lithography. Moreover, the presence of a diffusive background blurs the image and, thus, impairs the contrast and spatial resolution. The height of a microroughness of substrates of multilayer mirrors, which are used in the projection X-ray lithography, must not be higher than 0.2–0.1 nm (see Table 1). This requirement can be weaker in other applications of X-ray optics, but, in any case, the surface must be smooth at the wavelength scale; i.e., the roughness height should not exceed a few angstroms.

Table 1. Requirements to the accuracy of manufacturing mirrors for the projection X-ray lithography [60].

Spatial frequency	Required rms deviation/nm	Results obtained Europe EUCLIDES [61, 62]	USA ETS [63, 64]
$\infty - 1\ \mathrm{mm}^{-1}$	0.25	0.15–0.42	0.22–0.35
$1\ \mathrm{mm}^{-1} - 1\ \mu\mathrm{m}^{-1}$	0.20	0.15–0.40	0.15–0.22
$1\ \mu\mathrm{m}^{-1} - 50\ \mu\mathrm{m}^{-1}$	0.10	0.40	0.17–0.24

Note: in the cases of small and medium (high) spatial frequencies, we may speak about the surface shape and roughness, respectively.

The control of the substrate smoothness to this accuracy is an independent problem. Two setups, in which a technique of hard X-ray scattering was used, were built for solving this problem: by A.G. Tur'yanskii [65] at the LPI and by V.E. Asadchikov at the Institute of Crystallography of RAS [66]. The theory of this method was presented in [12, 67]. The results of measuring the correlation functions K of roughness heights shown in Fig. 6 allow one to compare the smoothness of substrates from different manu-

*The physical capabilities of multilayer optics were also implemented in practice through the obtainment of 'colour' X-ray imaging of the Sun. The Russian projects initiated at the LPI by S.L. Mandelshtam and I.A. Zhitnik in the mid-1970s were jointly accomplished by the LPI and Institute of Terrestrial Magnetism, Ionosphere, and Radio Wave Propagation (RAS) using the CORONAS satellites in 1994–2001 [51–53]. Being the director of the LPI, a member of the Presidium of the RAS, and a member of the Presidium of the Supreme Council of the USSR, N.G. Basov supported the development of this trend and promoted the financial support of the R&D.

**It is assumed that certain modifications of the existing technology and the use of excimer ArF (193 nm) and F_2 (157 nm) lasers as radiation sources will make it possible to achieve a miniaturisation level of 0.07 μm.

facturers. The smaller the correlation function, the smoother the surface. This function is equal to zero at all spatial frequencies for an ideally smooth surface. Table 2 presents another (integral) characteristic of actual substrates: the rms height of microroughnesses σ_{eff}.

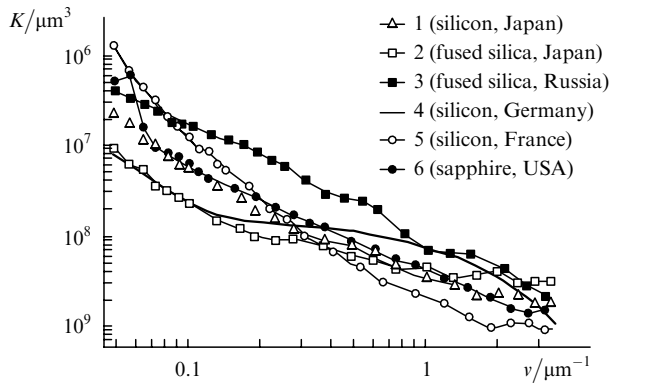

Figure 6. Correlation functions K of roughness heights for substrates processed by the deep grinding and polishing versus spatial frequency ν [31].

Table 2. Rms heights of microroughnesses of highly polished substrates of various materials in the range of spatial frequencies of $0.05-3.5\ \mu m^{-1}$ [68].

Substrate number	Sample	$\sigma_{\text{eff}}/\text{nm}$	Producert
1	Silcon	0.16	Japan
2	Fused silica	0.15	Japan
3	Fused silica	0.26	Russia
4	Silcon	0.16	Germany
5	Silcon	0.21	France
6	Saphire	0.18	USA

One can see from Table 2 that the method of hard X-ray scattering ensures the necessary accuracy of measuring the roughnesses of multilayer-mirror substrates for the projection X-ray lithography. It is also rather convenient for the development of the technology of polishing ultrasmooth surfaces (see details in [68]). As the radius of curvature of the studied surface increases, the specular reflection begins to mask the scattered radiation. In this case, it is possible to use a two-wave method based on a simultaneous measurement of the scattering indicatrices of the doublet components K_α and K_β of the copper characteristic line [69, 70]. Another possibility is to probe a rough surface using whispering-gallery modes in the hard X-ray region [41, 71].

Macroscopic deviations of the mirror surface shape from an ideal one directly influence the ray-optical and diffraction resolution. Consider the latter in more detail. For simplicity, let us analyse the reflection of a monochromatic wave by a flat mirror, which has a roughness of height h (Fig. 7). For the resolution of the optical system to be close to the diffraction limit, the phase distortion of the reflected wave at each optical element should be sufficiently small. The presence of a distortion is equivalent to a shift of a mirror segment by a value h, leading to the appearance of a phase factor $\exp(-i\Delta\varphi)$ in the reflectivity, where

$$\Delta\varphi = 2kh = \frac{4\pi h}{\lambda}. \tag{3}$$

By requiring that $\Delta\varphi$ should not exceed 0.25, we obtain $h < \lambda/50$. With $\lambda = 13$ nm, we find that, for mirrors used in the projection X-ray lithography, the deviation from an ideal shape should not exceed $2-3$ Å.

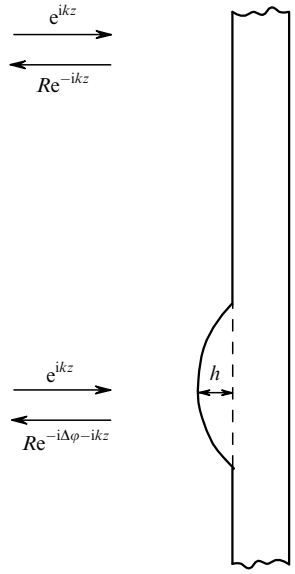

Figure 7. Local change in the reflectivity R upon a surface perturbation.

In order to monitor the reflectivity phase at $\lambda = 13$ nm, an interferometer installed at the ALS synchrotron in Berkeley (USA) was designed [72]. Nevertheless, the task of manufacturing mirrors with sufficiently precise shapes seems to be fairly difficult, because mirrors can be tested only after a coating is deposited (before the deposition, the reflectivities of substrates are too low). In order to overcome this difficulty, it was proposed to correct phase distortions of multilayer mirrors by etching their coatings [73]. The number of pairs of layers should be sufficiently large for the etching not to change the reflectivity magnitude.

Let us find the relation between the etching depth and the phase change. First, let us consider the change in the reflectivity phase $\delta\Phi$ upon etching off one period l. Because the number of periods is large, the removal of one period is equivalent to a mirror shift by l. In this case, it is obvious that the reflectivity does not change its magnitude but acquires a phase

$$\delta\Phi = 2kl. \tag{4}$$

Let us take into account the Bragg condition $l \approx \bar{\lambda}/2$, where $\bar{\lambda} = \lambda/\varepsilon^{1/2}$ is the wavelength in the medium [see (1)]. In this section, ε is the average value of the permittivity inside of the coating. By substituting $l = \lambda/2\varepsilon^{1/2}$ into (4), we obtain $\delta\Phi = 2\pi + \pi(1-\varepsilon)$. By omitting the insignificant term 2π in the phase, we have $\delta\Phi = \pi(1-\varepsilon)$. Thus, it is clear that, for an arbitrary etching depth h,

$$\delta\Phi = \frac{2\pi(1-\varepsilon)h}{\lambda}. \tag{5}$$

The comparison of (5) and (3) shows a significant difference between a multilayer and ordinary bulk mirror. In order to change the phase of a reflected wave by 0.25, a

layer with a thickness of $\lambda/50$ should be etched off an ordinary bulk mirror, and the corresponding thickness for a multilayer mirror is $2/(1-\varepsilon)$ times larger. In particular, at $\lambda = 13$ nm $(1-\varepsilon \approx 0.05)$, the thicknesses of the etched layers of bulk and multilayer mirrors are 0.25 and 10 nm, respectively. In the latter case, the problem is evidently more realistic.

If the dimensions of elements on a chip are sufficiently small, then, apart from the aforementioned factors of geometrical aberrations, diffraction, and inaccuracies in the manufacture of mirrors, an additional factor limiting the maximum spatial resolution of optical systems with multilayer mirrors should be taken into account. The matter is that such mirrors are not only wavelength-selective but also angular-selective elements; i.e., they reflect light only within a certain angular range. This naturally restricts the spatial frequencies (dimensions) of object parts transferred by the optical system. As was shown in [74], this effect is significant for wavelengths of 40–4 nm, if a resolution better than 0.06 μm is required.

At present, it is believed that most problems of X-ray optics for the projection X-ray lithography have been solved in principle, and only the cost of the instruments produced on its basis can be discussed. However, the problem of designing a reflecting mask and a radiation source, whose mean power at the operating wavelength should be 100–150 W, remains unsolved. Using the projection X-ray lithography, images of masks with 0.1-μm elements at a field of view of 24×32.5 mm, which corresponds to actual chip dimensions, were obtained on the ETS facility [63]. A level of 0.07 μm is expected to be reached in the nearest future. The elements of a four-mirror optical system for transferring images to the required accuracy were manufactured and tested [75]. A laser-plasma source based on an YAG laser with a mean power of 40 W was used in [63]. At the next stage, this power will be increased up to 1.7 kW. Electric-discharge X-ray sources are currently developed in parallel [76, 77]. Details of the state of this problem can be found in [23, 55, 63].

5. Multilayer mirrors for a repetitively pulsed X-ray laser

A sufficiently high pulsed and mean power of a capillary-discharge 46.9-nm laser [10] made it possible to perform experiments with coherent radiation at $\lambda < 100$ nm for the first time in a laboratory [11]. In order to use these potentialities to the highest degree, optical elements for controlling laser beams are required. The reflectivity of any material in this spectral range is no higher than 10 %. Therefore, we preferred to use multilayer structures. Proceeding from the discussion presented in Section 2, we selected pairs of Si and a transition metal with the unfilled 3*d*-shell, as promising materials for optical coatings for wavelengths of 35–50 nm [78]. The electronic configurations of these metals are listed in Table 3.

In transition metals, a competition between the 3*d*- and 4*s*-shell filling processes takes place. Because the 3*d*-shell in all these elements is unfilled, the $3p-3d$ transition from the inner 3*p*-shell is allowed. It is known that a strong resonance in the absorption spectra of all transition 3*d*-metals corresponds to this transition. However, direct measurements of $\mathrm{Im}\varepsilon$ and $\mathrm{Re}\varepsilon$ in the wavelength range of interest (30–50 nm) encounter difficulties for the reasons that will be discussed below. As to the experimental data on $\mathrm{Re}\varepsilon$, they are virtually absent.

Table 3. Basic electronic configurations of transition metals.

Element	Nucleus charge	Basic element configuration
Sc	21	$3p^6\,3d\,4s^2$
Ti	22	$3p^6\,3d^2\,4s^2$
V	23	$3p^6\,3d^3\,4s^2$
Cr	24	$3p^6\,3d^5\,4s$
Mn	25	$3p^6\,3d^5\,4s^2$
Fe	26	$3p^6\,3d^6\,4s^2$
Co	27	$3p^6\,3d^7\,4s^2$
Ni	28	$3p^6\,3d^8\,4s^2$

Let us use theoretical considerations. According to the reasonings in Section 2, a minimum absorption and, simultaneously, high $\mathrm{Re}\varepsilon$ values can be expected to the red from the resonance. This favours the obtainment of a high reflectivity of a multilayer mirror. The second component selected for the coating was Si, which has a low optical density in the wavelength range of interest. For this element, the values of $\mathrm{Re}(1-\varepsilon)$ and $\mathrm{Re}\varepsilon$ are small.

The analysis of the absorption spectra and calculations of $\mathrm{Im}\varepsilon$ and $\mathrm{Re}\varepsilon$ [78] made it possible to select a Sc–Si pair as the most suitable coating for the 46.9-nm line. The mirrors were manufactured at the Kharkov Polytechnical Institute and tested at the ALS (Berkeley) and BESSY (Berlin) synchrotron centres [79]. Fig. 8 shows the reflectivity of the Sc/Si mirror as a function of the angle of incidence at 46.9 nm. The mirror has a reflectivity of ~ 45 % and is optimised for the normal incidence. Such mirrors are currently used in various applications of capillary-discharge lasers: in interferometry, reflectometry, ellipsometry, tests of optical elements, material ablation, etc. [11].

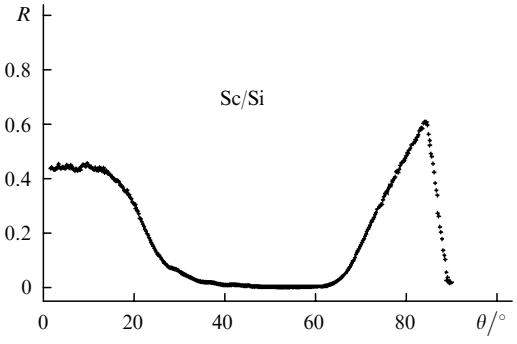

Figure 8. Reflectivity R of a Sc/Si mirror as a function of the angle of incidence θ measured with a 46.9-nm capillary-discharge X-ray laser.

The problem of synthesising multilayer coatings for the 35–50-nm region concerns not only lasers but has a wider significance. Earlier, there were no efficient reflectors in this spectrum region at all, while the radiation was used in synchrotron investigations and in solar physics. In particular, spectral lines lying between 40 and 42 nm are of interest for the diagnostics of the solar corona [80].

Turning to multilayer coatings, note that, as the wavelength increases to 30 nm, the reflectivity of a well-studied Mo–Si structure used at $\lambda \geqslant 13$ nm falls from 70 % to 20 %. The absence of an alternative is associated primarily with poor experimental data on the optical constants in the

range of 30 – 50 nm. Theoretical calculations also cannot still ensure the required accuracy.

A difficulty in measuring the optical constants in the range of 35 – 50 nm is associated with an extremely small depth of radiation penetration into any material. From this point of view, the range of 35 – 50 nm holds a record in the entire range of electromagnetic waves. This also concerns atmospheric gases, which, being adsorbed, contaminate the surfaces of the samples under study. Therefore, one is almost never sure that an experimental sample is sufficiently pure, and the results often depend on the sample preparation procedure [81]. Table 4 presents the data on the radiation penetration depth at $\lambda =$ 46.9 and 0.154 nm (Cu K_α) for various substances in two cases: the normal incidence,

$$l_{\rm ni} = \frac{\lambda}{4\pi\kappa}, \tag{6}$$

and a grazing incidence at the critical angle,

$$l_{\rm ca} = \frac{\lambda}{4\pi(n\kappa)^{1/2}}, \tag{7}$$

where $n + i\kappa = \varepsilon^{1/2}$.

Table 4. Penetration depths in various materials for 46.9-nm laser radiation and 0.154-nm radiation of an X-ray tube.

Material	$l_{\rm ni}$/nm		$l_{\rm ca}$/nm	
	$\lambda = 46.9$ nm	$\lambda = 0.154$ nm	$\lambda = 45.9$ nm	$\lambda = 0.154$ nm
C	5.1	766×10^3	6.0	97.0
Si_3N_4	9.3	74×10^3	7.1	30.2
SiO_2	11.7	130×10^3	8.3	40.0
SiC	16.0	70×10^3	11.0	30.0
Si	129	80×10^3	27.0	32.0
InP	41.5	11×10^3	13.0	11.5
GaAs	62.0	28×10^3	17.0	5.9
Ir	7.0	2×10^3	5.7	5.4

One can see from Table 4 that for some elements, including all the atmospheric gases, which precipitate on surfaces directly or in the form of compounds, the 46.9-nm radiation penetrates to a depth of at most 10 nm. This extremely complicates optical measurements. In fact, all modern methods for determining optical constants (reflectometry and ellipsometry) in the VUV and soft X-ray regions are related to measurements of the reflectivity. Subsequently, the Fresnel formulas are used to express the optical constants in terms of the measured reflectivity or utilising $\mathrm{Re}\,\varepsilon$ and $\mathrm{Im}\,\varepsilon$ as fitting parameters for the experimental curves. However, due to a contamination of the sample surface, the Fresnel formulas implying a stepwise change in ε at interfaces are inapplicable. The true distribution of the permittivity near the surface is unknown, and, thus, a numerical solution of the wave equation is also inapplicable. Attempts to overcome this difficulty by a surface purification and treatment were made in [82, 83]. Corrections of an order of λ/d to the Fresnel formulas, where d is the thickness of an arbitrarily-shaped transition layer, were found in [84, 85]. However, none of these approaches gives an exhaustive solution to the problem of sample-surface contamination during measurements of optical constants in the VUV and soft X-ray regions.

Probably, a way out is the method proposed in [86], which is based on measuring the transmission and reflectivity of a series of protected films deposited onto a substrate. In this case, it becomes possible to exclude the influence of transition and atmosphere-contaminated layers and to extract the optical material constants from the experimental data. The results for Sc obtained in this way and shown in Fig. 9 were used for calculating and synthesising Sc/Si multilayer coatings in the 35 – 45-nm range. The results of calibrations of diffraction gratings, which are replicas of a 3600-lines mm^{-1} grating mounted at the Skylab space station, for these wavelengths are published in [87]. A Sc/Si coating was deposited on the grating surfaces for enhancing the calibration efficiency. As a result, the efficiency of gratings became three times higher.

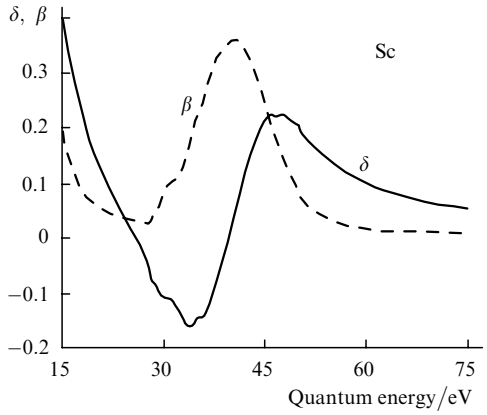

Figure 9. Optical constants for scandium at wavelengths of 60 – 17 nm ($\delta = 1 - \mathrm{Re}\,\varepsilon$, $\beta = \mathrm{Im}\,\varepsilon$).

6. Conclusions

A single review cannot embrace all the problems of physics, technology, and applications of modern multilayer X-ray optics. We have mainly considered the works that were performed at the Department of Quantum Radiophysics headed by N.G. Basov or those concerned with the topics of its studies. Several trends are developed at other Departments of the LPI, as well as at the Institute of Microstructure Physics (Nizhnii Novgorod), Institute of Nuclear Physics (Novosibirsk), Institute of Microelectronic Technology and Extra-Pure Materials, (Chernogolovka), Moscow Institute of Physics and Technology, Moscow Institute of Electronic Machine Building, and other research centres. It is obvious that multilayer X-ray optics will contribute to the further mastering of the short-wavelength region in laser physics to which N.G. Basov devoted his activity.

Acknowledgements. The author is grateful to Yu.S. Kas'yanov and A.N. Starodub for comments and to F. Shaefers for presenting the data of mirror reflectivity measurements. This work was supported by the Integratsiya Program (Grant Nos I0859 and V0056) and the CRDF Grant No. RP1-2267.

References

1. Basov N.G., Krokhin O.N. *Zh. Eksp. Teor. Fiz.*, **46**, 171 (1964).
2. Rozanov V.B. *Kvantovaya Elektron.*, **24**, 1095 (1997) [*Quantum Electron.*, **27**, 1063 (1997)].
3. Basov N.G., Zakharenkov Yu.A., Rupasov A.A., Sklizkov G.V., Shikanov A.S. *Diagnostika plotnoi plazmy* (Dense Plasma Diagnostics) (Moscow: Nauka, 1989).
4. Boiko V.A., Vinogradov A.V., Pikuz S.A., Skobelev I.Yu., Faenov A.Ya. *X-ray Spectroscopy of Laser Plasma, Itogi Nauk. Tekh., Ser. Radiotekh.* (Moscow: VINITI, 1980) Vol. 27.
5. Jaegle P., Carillon A., Dhez P., Jamelot G., Sureau A., Cukier M. *Phys. Lett. A*, **36**, 167 (1971).
6. Molchanov A.G. *Usp. Fiz. Nauk*, **106**, 165 (1972).
7. Vinogradov A.V., Zel'dovich B.Ya. Preprint FIAN (185) (Moscow, 1976); *Appl. Opt.*, **16**, 89 (1977).
8. Vinogradov A.V., Sobelman I.I., Yukov E.A. *J. Physique. Coll. C4*, **39**, C4-61 (1978).
9. Spiller E. *Appl. Phys. Lett.*, **20**, 365 (1972).
10. Benware B.R., Macchietto C.D., Moreno C.H., Rocca J.J. *Phys. Rev. Lett.*, **81**, 5804 (1998).
11. Vinogradov A.V., Rocca J.J. *Kvantovaya Elektron.*, **33**, 7 (2003) [*Quantum Electron.*, **33**, 7 (2003)].
12. Vinogradov A.V., Brytov I.A., Grudskii A.Ya., Kogan M.T., Kozhevnikov I.V., Slemzin V.A. *Zerkal'naya rentgenovskaya optika* (X-ray Mirror Optics) (Leningrad: Mashinostroenie, 1989).
13. Kozhevnikov I.V. *Theory of Reflecting X-ray Optical Elements for Controlling Soft X-ray Beams*, Cand. Diss. (Moscow, LPI, 1987).
14. Yamamoto M., Namioka T. *Appl. Opt.*, **31**, 1622 (1992).
15. Salashchenko N.N. *Poverkhnost*, (1), 50 (1999).
16. Vinogradov A.V., Tolstikhin O.I. *Trudy FIAN*, **196**, 168 (1989); Tolstikhin O.I., Vinogradov A.V. *Appl. Phys. B*, **50**, 213 (1990).
17. Tolstikhin O.I. *Theory of Dynamic Polarisability of Multielectron Atoms and Ions*, Cand. Diss. (Moscow, LPI, 1991).
18. Tolstikhin O.I., Vinogradov A.V. *Phys. Rev. Lett. A*, **45**, R7667 (1992).
19. Artyukov I.A., Zelentsov V.V., Krymskii K.M. Preprint FIAN (14) (Moscow, 2000); *X-ray Sci. Technol.* (2002) (in press).
20. Shaefers F. *Physica B*, **283**, 119 (2000).
21. Gluskin E.S., Gaponov S.V., Dhez P., Ilyinsky P.P., Salashenko N.N., Shatunov Y.M., Trakhtenberg E.M. *Nucl. Instr. Meth. A*, **246**, 394 (1986).
22. Alexandrov Yu.M., Vinogradov A.V., Zorev N.N., Kozhevnikov I.V., Kondratenko V.V., Koshevoi M.O., Murasheva V.A., Rupasov A.A., Fedorenko A.I., Shikanov A.S., Yakimenko M.N. *Nucl. Instr. Meth. A*, **282**, 551 (1989).
23. Attwood D.T. *Soft X-Ray and Extreme Ultraviolet Radiation: Principles and Applications* (Oxford University Press, 2000).
24. Henke B.L., Gullikson E.M., Davis J.M. *Atomic Data and Nuclear Data Tables*, **54**, 181 (1993).
25. Vinogradov A.V. (Ed.) *X-ray Optics and Surface Science. CIS Selected Paper* (USA, Bellingham: SPIE Opt. Eng. Press, 1995) V. 2453.
26. Kondratenko V.V., Pershin Yu.P., Poltseva O.V., Fedorenko A.I., Zubarev E.N., Yulin S.A., Kozhevnikov I.V., Sagitov S.I., Chirkov V.A., Levashov V.E., Vinogradov A.V. *Appl. Opt.*, **32**, 1811 (1993).
27. Vinogradov A.V., Pershin Yu.P., Zubarev E.N., Voronov D.L., Pen'kov A.V., Kondratenko V.V., Uspenskii Yu.A., Artioukov I.A., Seely J.F. *Proc. SPIE Int. Soc. Opt. Eng.*, **4505**, 230 (2001).
28. Bugaev E.A., Zubarev E.N., Kondratenko V.V., Fedorenko A.I. *Trudy natsion. konf. po primeneniyu rentgenovskogo, sinkhrotronnogo izluchenii, neitronov i elektronov dlya issledovaniya materialov (RSNE'97)* [Proc. National Conf. on the Application of X-ray and Synchrotron Radiations, Neutrons, and Electrons for Investigations of Materials (XSNE'97)] (Dubna, 1997) Vol. 2, p. 268.
29. Kondratenko V.V. *Phase and Structural Transformations in Nanometer-Size X-ray Optical Multilayer Compositions*, Doct. Diss. (Kharkov, Kharkov Polytechnical Institute, 1999).
30. Bugaev E.A. *Formation, Structure, and Thermal Failure of Ni/C, Cr/C, Cr_3C_2/C, CrB_2/C, and TiC/C Multilayer Film Systems*, Cand. Diss. (Kharkov, Kharkov Polytechnical Institute, 1999).
31. Spiller E. *Soft X-Ray Optics* (Bellingham: SPIE Opt. Eng. Press, 1994).
32. Fischer D.A., Sambasivan S.A., Kuperman A., Platonov Y., Wood J.L. *Synchrotron Radiation News*, **15** (3), 16 (2002).
33. Vinogradov A.V., Elinson V.M., Ivanivskii G.F., Kozhevnikov I.V., Sagitov S.I., Sleptsov V.V. *Opt. Spektrosk.*, **59**, 703 (1985).
34. Arkadiev V., Baranov A., Erko A., Kondrashov P., Langhoff N., Novoselova E., Smirnov I., Veldkamp M., Packe I. *Proc. SPIE Int. Soc. Opt. Eng.*, **3773**, 122 (2000).
35. Balakireva L.L. *Theoretical Investigations of Optical Properties of Artificial Multilayer Structures in the Soft X-ray Region*, Cand. Diss. (Dolgoprudnyi, Moscow Physicotechnical Institute, 1994).
36. Pirozhkov A.S. *Wide-Band Spectral Instruments Based on Multilayer X-ray Optics,* Diploma Work (Dolgoprudnyi, Moscow Physicotechnical Institute, 1999).
37. Bukreeva I.N., Kozhevnikov I.V., Zigler E. *Proc. SPIE Int. Soc. Opt. Eng.*, **3448**, 322 (1998).
38. Kozhevnikov I.V., Bukreeva I.N., Ziegler E. *Nucl. Instr. Meth. A*, **460**, 424 (2001).
39. Alred D.D., Turley R.S., Squires M.B. *Proc. SPIE Int. Soc. Opt. Eng.*, **3767**, 280 (2000).
40. Kozhevnikov I.V. Preprint FIAN (3) (Moscow, 2002).
41. Bukreeva I.N. *Theoretical Investigations of Wideband X-ray Optical Elements and Systems*, Cand. Diss. (Moscow, Moscow Engineering Physics Institute, 2002).
42. Artioukov I.A., Fedorenko A.I., Kondratenko V.V., Yulin S.A., Vinogradov A.V. *Opt. Commun.*, **102**, 401 (1993).
43. Artyukov I.A., Asadchikov V.E., Vinogradov A.V., Kas'yanov Yu.S., Kondratenko V.V., Serov R.V., Fedorenko A.I., Yudin S.A. *Kvantovaya Elektron.*, **22**, 951 (1995) [*Quantum Electron.*, **25**, 919 (1995)].
44. Artioukov I.A., Asadchikov V.E., Vinogradov A.V., Kasyanov Yu.S., Kondratenko V.V., Serov R.V., Fedorenko A.I., Yulin S.A. *Opt. Lett.*, **20**, 2451 (1995).
45. Artioukov I.A., Krymski K.M. *Opt. Eng.*, **39**, 2163 (2000).
46. Artyukov I.A. *Reflection X-ray Optics for Microscopy and Lithography*, Cand. Diss. (Moscow, LPI, 1992).
47. Krymskii K.M. *Optimised Optical Systems and Reflecting Coatings for Soft X Rays*, Cand. Diss. (Dolgoprudnyi, Moscow Physicotechnical Institute, 2000).
48. Artyukov I.A., Asadchikov V.E., Vilenskii A.I., Vinogradov A.V., Zagorskii D.L., Levashov V.E., Mchedlishvili B.V., Popov A.V., Postnov A.A., Struk I.I. *Dokl. Akad. Nauk*, **372**, 608 (2000).
49. Postnov A.A. *Development of Methods of X-ray Microscopy for Studying Biological and Polymer Objects*, Cand. Diss. (Moscow, Institute of Crystallography RAS, 1999).
50. Handy B.N., Acton L.W., Kankelborg E.C., et. al. *Solar Phys.*, **187**, 229 (1999).
51. Oraevsky V.N., Sobel'man I.I., Zhitnik I.A., Kuznetsov Vl.D. *Usp. Fiz. Nauk*, **172** (8), 949 (2002).
52. Zhitnik I.A., Bugaenko O.I., Ignat'ev A.P. *Mon. Not.*, **338**, 67 (2002).
53. Oraevsky V.N., Sobel'man I.I. *Pis'ma Astron. Zh.*, **78** (6), 457 (2002).
54. Korendyke C., Brown C., Seely J. *SPIE's OEmagazine*, August, 23 (2002).
55. Stulen R.H., Sweeney D.W. *IEEE J. Quantum Electron.*, **35**, 694 (1999).
56. *Poverkhnost*, (1) (1998), (1) (1999), (1) (2000), (1) (2001), (1) (2002).
57. Vinogradov A.V., Zorev N.N. Preprint FIAN (104) (Moscow, 1987); Vinogradov A.V., Zorev N.N. *Dokl. Akad. Nauk*, **302**, 82 (1988).
58. Zorev N.N. *Trudy FIAN*, **196**, 129 (1989).
59. Artyukov I.A., Balakireva L.L., Biikerk F., Vinogradov A.V., Zorev N.N., Kozhevnikov I.V., Kondratenko V.V., Ogurtsov O.F., Ponomarenko A.G., Fedorenko A.I. *Kvantovaya Elektron.*, **19**, 114 (1992) [*Quantum Electron.*, **22**, 99 (1992)].

60. Levinson H.J. *Principles of Lithography* (Bellinghaim: SPIE Opt. Eng. Press, 2001).
61. Benschop J.P., van Dijesseldonk A.J.J., Kaiser W.M. *J. Vac. Sci. Technol. B*, **17** (6), 2978 (1999).
62. Meiling H., Benschop J., Dinger U., Kurz P. *Proc. SPIE Int. Soc. Opt. Eng.*, **4343**, 38 (2001).
63. Tichenor D.A., Ray-Chaudhuri A.K. et al. *Proc. SPIE Int. Soc. Opt. Eng.*, **4506**, 9 (2001).
64. Gullikson E.M., Mrowka S., Kaufmann B.B., *Proc. SPIE Int. Soc. Opt. Eng.*, **4343**, 363 (2001).
65. Kiseleva K.V., Tur'yanskii A.G. Preprint FIAN (34) (Moscow, 1979).
66. Alautdinov B.M., Artyukov I.A, Asadchikov V.E., Karabekov A.Yu., Kozhevnikov I.V. *Kristallografiya*, **39**, 605 (1994).
67. Vinogradov A.V., Zorev N.N., Kozhevnikov I.V., Sagitov S.I., Tur'yanskii A.G. *Zh. Eksp. Teor. Fiz.*, **94**, 203 (1998).
68. Asadchikov V.E., Vinogradov A.V., Kozhevnikov I.V., Krivonosov Yu.S., Sagitov S.I., Mersier H., Namba M., Yamomoto M. *Zavod. Labor.*, **67** (12), 19 (2001).
69. Tur'yanskii A.G., Vinogradov A.V., Pirshin I.V. *Prib. Tekh. Eksp.*, (1), 105 (1999).
70. Popov N.L., Uspenskii Yu.A., Tur'yanskii A.G., Vinogradov A.V. *Poverkhnost* (2003) (in press).
71. Asadchikov V.E., Bukreeva I.N., Vinogradov A.V., Kozhevnikov I.V., Ostashev V.I., Sagitov S.I. *Kvantovaya Elektron.*, **24**, 845 (1997) [*Quantum Electron.*, **27**, 824 (1997)].
72. Nalleau P., Goldberg K.A., Gullikson E.M., Bokor J. *J. Vac. Sci. Technol. B*, **17** (6), 2987 (1999).
73. Yamamoto M. *Nucl. Instr. Meth.*, **467**, 1282 (2001).
74. Artioukov I.A., Fetchenko R.M., Vinogradov A.V. *J. Opt. A: Pure and Appl. Opt.*, **4**, 233 (2002).
75. Souflie R., Spiller E., Schmidt M.A., et al. *Proc. SPIE Int. Soc. Opt. Eng.*, **4343**, 51 (2001).
76. Sobel'man I.I., Shevel'ko A.P., et al. *Kvantovaya Elektron.*, **33**, 3 (2003) [*Quantum Electron.*, **33**, 3 (2003)].
77. Banine V., Moores R. *Proc. SPIE Int. Soc. Opt. Eng.*, **4343**, 203 (2001); Stamm U., Ahmad I., Borisov V.M., et al. *Proc. SPIE Int. Soc. Opt. Eng.*, **4688**, 626 (2002).
78. Uspenskii Yu.A., Antonov S.V., Fedotov V.Yu., Vinogradov A.V., *Proc. SPIE Int. Soc. Opt. Eng.*, **3156**, 288 (1997).
79. Uspenskii Yu.A., Levashev V.E., Vinogradov A.V., Fedorenko A.I., Kondratenko V.V., Persin Yu.P., Zubarev E.N., Fedotov V.Yu. *Opt. Lett.*, **23**, 771 (1998).
80. Feldman U. *Phys. Scripta*, **46**, 202 (1992).
81. Palik E.D. *Handbook of Opt. Constants of Solids* (San Diego, California: Academic, 1985).
82. Soufli R., Gullikson E.M. *Appl. Opt.*, **37**, 1713 (1998).
83. Artioukov I.A., Benware B.R., Rocca J.J., Forsyth M., Uspenskii Yu.A., Vinogradov A.V. *IEEE J. Selected Topics in Quantum Electron.*, **5**, 1495 (1999).
84. Fetchenko R.M., Vinogradov A.V. *Opt. Lett.*, **25**, 1 (2000).
85. Fetchenko R.M., Popov A.V., Vinogradov A.V. *J. Russian Laser Research*, **22**, 139 (2001).
86. Uspenskii Yu.A., Seely J.F., Popov N.L., Vinogradov A.V., Persin Yu.P., Kondratenko V.V. *VI Intern. Conf. Phys. of X-Ray Multilayer Structures* (Chamonix, Grenoble, 2002) p. 6.
87. Seely J.F., Uspenskii Yu.P., Kondratenko V.V., Vinogradov A.V. *Appl. Opt.*, **41**, 1846 (2002).
88. Akhsakhalyan A.D. *Formation of Surfaces of Specified Profiles by the Methods of Thermoplastic and Elastic Bending and Deposition of Multilayer Nanostructures on Them for X-ray Control Systems*, Cand. Diss. (N. Novgorod, Institute of Microstructure Physics, 2002).

N.G. Basov in the late 1960s.